COASTAL ENGINEERING JOURNAL
2018, VOL. 60, NO. 4, 484–498
https://doi.org/10.1080/21664250.2018.1529265

ORIGINAL RESEARCH PAPER

Tidal bore hydrodynamics and sediment processes: 2010–2016 field observations in France

David Reungoat[a], Pierre Lubin [a], Xinqian Leng [b] and Hubert Chanson [b]

[a]CNRS, Université de Bordeaux, Pessac, France; [b]School of Civil Engineering, The University of Queensland, Brisbane, Australia

ABSTRACT

A tidal bore is a compressive wave, advancing upstream in an estuary when the flood tidal flow starts. It is observed when a macro-tidal flood flow enters the funnel shaped river mouth with shallow waters. Its upriver propagation impacts the natural system, with sediment scouring and suspension. The tidal bores of the Garonne and Sélune Rivers in France were extensively investigated between 2010 and 2016. Instantaneous velocity measurements were conducted continuously at high-frequency (50 to 200 Hz) during each bore event. In the Garonne River, instantaneous sediment concentration data were obtained and the sediment properties were systematically tested. The nature of the observations was comprehensive, regrouping hydrodynamics and turbulence, sedimentology and suspended sediment transport. The key outcomes show that the tidal bore occurrence has a marked effect on the velocity field and suspended sediment processes, including a sudden flow deceleration and flow reversal during the bore passage. The turbulent Reynolds stresses present large instantaneous amplitudes, with rapid fluctuations, during the tidal bore. The sediment flux data imply considerable mass transport rates during the first hour of flood tide. This unique review of field data further shows a number of common features, as well as the uniqueness of each individual event.

ARTICLE HISTORY
Received 3 December 2017
Accepted 7 September 2018

KEYWORDS
Tidal bores; field measurements; hydrodynamics; turbulence; sediment processes; France

1. Introduction

While laboratory experiment could generate specific "unnatural" flow, nature can create some unlogical flow phenomena that may occur under specific conditions. Tidal bore is one of these famous unexpected phenomena: a wave front that flow against the initial mean stream of a river. A tidal bore is basically a water surface discontinuity, i.e. compression wave, propagating upstream in the estuary (Figure 1). It may take place under large tidal range conditions, in a funnel-shaped estuary which bathymetry amplifies the energy of the tide flowing upstream against the river flow. A hydrodynamic shock then occurs, generating a bore propagating inland as the river flow reverses upstream, behind the compression wave (Lynch, 1982; Chanson, 2011a). Historically, the best documented tidal bores have been those of the Seine River (France) and Qiantang River (China). Although it no longer exists in its most energetic and spectacular form, the "*mascaret*" (tidal bore) of the Seine River was documented first during the seventh and ninth centuries AD (Malandain, 1988). Records of the Qiantang River bore may be traced back to the seventh and second centuries BC, with further writing from the eighth century (Moule, 1923) (Figure 1(a,b)). Another famous tidal bore is the "*pororoca*" of the Amazon River (Brazil), first reported by PINZON and LA CONDAMINE during the sixteenth and eighteenth centuries, respectively (de La Condamine, 1745; Manzano Manzono and Manzano Fernandez Heredia 1988). The Hooghly bore (Ganga River in India) was described in the nineteenth century historical nautical reports and is still active. Smaller tidal bores occur on the Severn River near Gloucester (UK), on the Garonne and Dordogne Rivers (France), and on the Bay of Fundy (Canada). Worldwide, about 300 to 450 shallow-water bays, estuaries, and rivers are influenced by tidal bores (Bartsch-Winkler and Lynch, 1988; Chanson, 2011a).

The upstream propagation of tidal bores may span over long distance and has a significant influence on the natural systems. Figure 1(a,b) illustrates the impact of tidal bores on artificial structures. While tidal bore surfing has become an extreme sport in a number of rivers (Figure 1(e,f)), other bores have had ominous reputations, e.g. the Seine and Qiantang River bores. Along the Qiantang River, numerous tidal bore warning signs are erected (Figure 2), with over 80 drownings in the bore for the past two decades (Pan and Chanson, 2015). The French novelist Jules Vernes described the terrifying impact of tidal bore: "*pororoca, this terrifying tidal bore that, for three days before the new or full moon, takes only two minutes, instead of six hours, to rise the flood tide*

CONTACT David Reungoat h.chanson@uq.edu.au

Figure 1. Tidal bore photographs.

(a) Tidal bore of the Qiantang River at Yanguan (China) on September 23 2016 about 16:00 – note the bore impact onto the Qiantang River Bore Observation Station
The vertical sluice gate structure – Jiuxi is located about 58 km upstream of Yanguan
(c) Tidal bore of the Sélune River at La Roche Torin, Bay of Mt St Michel (France) on April 7 2004
(d) Tidal bore of the Sélune River at Pontaubault, Bay of Mt St Michel (France) on April 7 2004 – Pontaubault is located 7.5 Km upstream of La Roche Torin and the tidal bore arrived 51 min later on that day
(e) Undular tidal bore of the Dordogne River at Port de St Pardon (France) on September 27 2008 afternoon – note the kayakists on in front of second wave crest and the surfer riding ahead of the third wave crest
(f) Undular tidal bore along the Canal à la Mer between Port de Brevands and Carentan (France) on May 19 2015 about 21:15

water elevation of about 4–5 m above the low water level. It is a real tsunami, terrible among all." (Vernes, 1881)

The bore propagation provokes intense sediment transport, linked to erosion, solid suspension, and upwelling (Greb and Archer, 2007; Chanson et al., 2011; Keevil, Chanson, and Reungoat, 2015; Furgerot et al., 2016) as well as interactions with sediment bed forms (Keevil. 2016; Reungoat, Leng, and Chanson, 2017b). The flow field behind the tidal bore advects very high suspended sediment concentrations (SSCs), with observed concentrations in excess of 40 kg/m^3 (Fan et al., 2014; Reungoat, Leng, and Chanson, 2017). In cohesive sediment estuarine and coastal zones, the erosional and scouring processes leading to landforms modifications are functions of the rheological characteristics of the sediment deposits (Faas, 1995; Keevil, Chanson, and Reungoat, 2015). Field observations in tidal bores hinted a two-stage bed scour mechanism at each event: first surface bed erosion in the form of surface peeling, followed by delayed mass erosion (Pouv et al., 2014; Reungoat, Leng, and Chanson, 2017).

At present, *in situ* tidal bores' measurements are relatively rare and scarce data are available. Early observations in China, France, and UK mentioned the bore

Figure 2. Tidal bore warning sign along the Qiantang River at Laoyanchang (China) on September 23 2016, with a policeman behind the sign (far right).

shape and arrival time. The earliest detailed measurements are possibly those of Partiot in the Seine River, including water elevations and float speeds (Partiot, 1861; Bazin, 1865). In the last 50 years, a limited number of field studies were conducted. Table 1 presents a summary. All studies emphasized the massive impact of the bore passage. In several cases, substantial losses of equipment and damage to instrumentation were reported (Kjerfve and Ferreira, 1993; Simpson, Fisher, and Wiles, 2004; Wolanski et al., 2004).

The tidal bore of the Garonne River (France) was comprehensively investigated between 2010 and 2016 as part of the Project Mascaret ANR-10-BLAN-0911. In addition, a field study was investigated in the Sélune River (France). The nature of the field observations was thorough, including hydrodynamics and turbulence, suspended sediment transport, and sedimentology. The aim of the paper is to review the key outcomes of the project, spanning over several years of observations and measurements, as well as developing a basic understanding of tidal-bore-affected estuarine zones in terms of temporal evolution of suspended sediment processes correlated to hydrodynamics, based upon large-scale field observations. A review of field data further shows a number of features common to all tidal bores, as well as some unique characteristics of each individual event.

2. Field deployments

2.1. In situ *experiments in macro-tidal estuaries*

Field measurements were conducted in two different systems in France, with semi-diurnal tides: the Garonne River upstream of Bordeaux and the Sélune River at Pointe du Grouin du Sud, Bay of Mt St Michel. The first site was the Arcins channel (Figure 3(a)) about 102 km upstream of the river mouth. The Arcins channel is 1.8 km long and 70 m wide, and the water depth is about 1.1–2.5 m at low tide (Figure 4(a)). The second site was located at the end of the Bay, about 500 m downstream of the confluence of the Sélune and Sée Rivers. The channels in the Bay change with time. During the field study, the main channel is about 35 m wide, with less than 0.5 m water depth at low tides, while the flood tide flow submerged all the sand banks, the channel width exceeding 2 km during the flood and early ebb tide (Figures 3(b) and 4(b)). Figure 3 presents photographs of the sites and Figure 4 shows the surveyed cross sections, looking downstream.

Field observations took place predominantly during spring tides. All field deployments took place between June and November, when the river water levels were relatively low. Table 2 summarizes the site, dates, and tidal range (Columns 2, 3, and 4). In Table 2, the initial water depth is listed in Column 9 (prior to the tidal bore passage).

2.2. *Instrumentation*

Free-surface elevations were recorded using a survey staff, placed 2 m away from the velocimeter to minimize any form of interference. During each bore passage, a video camera was used to record the rapid change in water levels. The instantaneous velocities were recorded with an acoustic Doppler velocimeter (ADV) sampled continuously at a frequency of 50–200 Hz depending upon the field deployment. The ADV recordings started more than 1 h before

Table 1. Detailed field measurements in tidal bores.

Reference	Initial flow V_1 m/s	d_1 m	Instrument	Channel geometry	Remarks
Lewis (1972)	0 to +0.2	0.9–1.4	Hydro-Products™ type 451 current meter	Dee River (UK) near Saltney Ferry footbridge. Trapezoidal channel	Field experiments between March and September 1972.
Navarre (1995)	0.65–0.7	1.12–1.15	Meerestechnik-Electronik GmbH model SM11J acoustic current meter (sampling: 10 Hz)	Dordogne River (France) at Port de Saint Pardon Width ~290 m	Field experiments on April 25 and 26 1990.
Kjerfve and Ferreira (1993)			Interocean™ S4 electromagnetic current meters (sampling: 1–2 Hz)	Rio Mearim (UK)	Field experiments on August 19– 22 1990 and January 28–February 2 1991.
Simpson, Fisher, and Wiles (2004)	0.1	~0.8	ADCP (1.20 MHz) (sampling rate: 1 Hz)	Dee River (UK) near Saltney Ferry Bridge. Trapezoidal channel (base width ~60 m)	Field experiments in May and September 2002.
Wolanski et al. (2004)	0.15	1.5–4	Nortek™ Aquadopp ADCP (sampling: 2 Hz)	Daly River (Australia). Width ~140 m	Field experiments in July and September 2002, and on July 2 2003.
Fan et al. (2012)	–	–	ADCP (1.2 MHz)	Daquekou, Qiantang River (China)	Field experiments from April 30 to May 2 2010.
Furgerot et al. (2013)	0.4	0.75	ADV Nortek™ Vector (6 MHz) (sampling: 64 Hz)	Sée River (France) Width ~22 m	Undular bore on May 7 2012.
Xie and Pan (2013)	2–2.8	2.0	ADCP	Yanguan, Qiantang River (China) Width ~2–3 km	Field experiments on October 10 and 11 2010.
Keevil (2016)	0.05–0.6	~1.8 m	ADCP Teledyne RDI Rio Grande (1.2 MHz) (sampling:1 Hz) & Midas ECM current meter	Longney Sands, Severn River (UK)	Field experiments on September 9 2014.
Tu and Fan (2017)	–	–	ADV Nortek™ Vector (6 MHz) (sampling: 64 Hz) & ADCP Teledyne RDI (1.20 MHz) (sampling: 0.1 Hz)	Daquekou, Qiantang River (China)	Field experiments on October 16–25 2012.
Mascaret project					
Mouaze, Chanson, and Simon (2010)	0.86–0.59	0.15–0.11*	ADV Nortek™ Vector (6 MHz) (sampling: 64 Hz)	Pointe du Grouin du Sud, Sélune River (France)	Breaking tidal bores. September 24 and 25 2010.
Chanson et al. (2011)	0.33–0.30	1.40–1.43*	ADV Nortek™ Vector (6 MHz) (sampling: 64 Hz)	Arcins channel, Garonne River (France) Width ~76 m	Undular tidal bores. September 10 and 11 2010.
Reungoat, Chanson, and Caplain (2014)	0.68–0.59	2.0–1.94*	microADV Sontek™ (16 MHz) (sampling: 50 Hz)		Weak undular tidal bores. June 7 2012.
Keevil, Chanson, and Reungoat (2015)	0.26	1.32*	ADV Nortek™ Vectrino+ (10 MHz) (sampling: 200 Hz)		Undular tidal bore on October 19 2013.
Reungoat, Leng, and Chanson (2017)	0.18–0.29	0.87–1.50*	ADV Nortek™ Vectrino+ (10 MHz) (sampling: 200 Hz)		Undular tidal bores. August 29–September 1 2016 and October 27 2015
Reungoat, Leng, and Chanson (2017b)	0.07–0.09	1.7*	ADV Nortek™ Vectrino+ (10 MHz) (sampling: 200 Hz)		Undular tidal bores. November 14 and 15 2016

d_1: initial water depth (at sampling location); V_1: initial flow velocity; –: information not available; *: equivalent depth A_1/B_1.

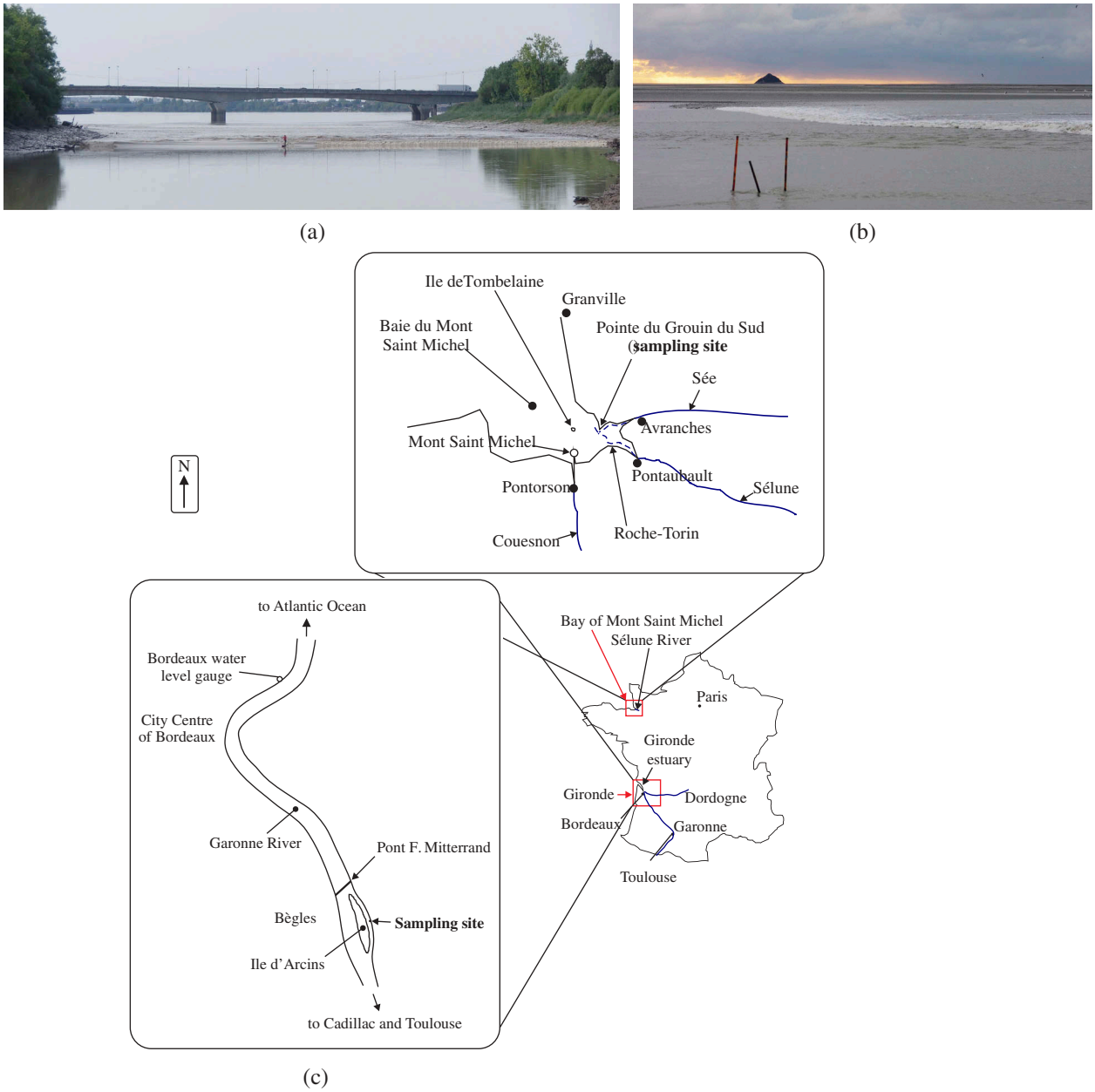

Figure 3. Photographs of field experimental sites.

(a) Garonne River tidal bore in the Arcins channel (France) on August 31 2015 afternoon
(b) Sélune River tidal bore at La Pointe du Grouin du Sud, Bay of Mt St Michel (France) on September 24 2010 evening – La Pointe du Grouin du Sud is located 2 Km upstream of La Roche Torin
(c) Map of France and sketches of the channels of the Garonne and Sélune Rivers

the bore passage and continued for more than 1 h after the bore passage. All the ADV data were rigorously post-processed to eliminate any wrong and spurious data.

In the Garonne River, water samples were collected at low tide on most days, for sediment bed and sediment-laden investigations. The bed material was composed of about 80% silt. Samples were analyzed in terms of material density, granulometry, and rheometry using a well-established protocol (Chanson et al., 2011; Keevil, Chanson, and Reungoat, 2015). The ADV unit was calibrated as a function of SSC against known, artificially produced diluted concentrations of material collected on bed site and thoroughly mixed. The SSC estimates were successfully compared to water sample data (Keevil, Chanson, and Reungoat, 2015; Reungoat, Leng, and Chanson, 2017).

3. Observations

In the Arcins channel, the tidal bore formed at the entrance of the channel, i.e. the northern end (Figure 3(c)). The bore propagated as a breaking surge across the entire river width, initially, as it advanced over a very shallow bar consisting of gravel, sand, and mud. As the bore advanced, it became an undular bore owing to the deeper bathymetry

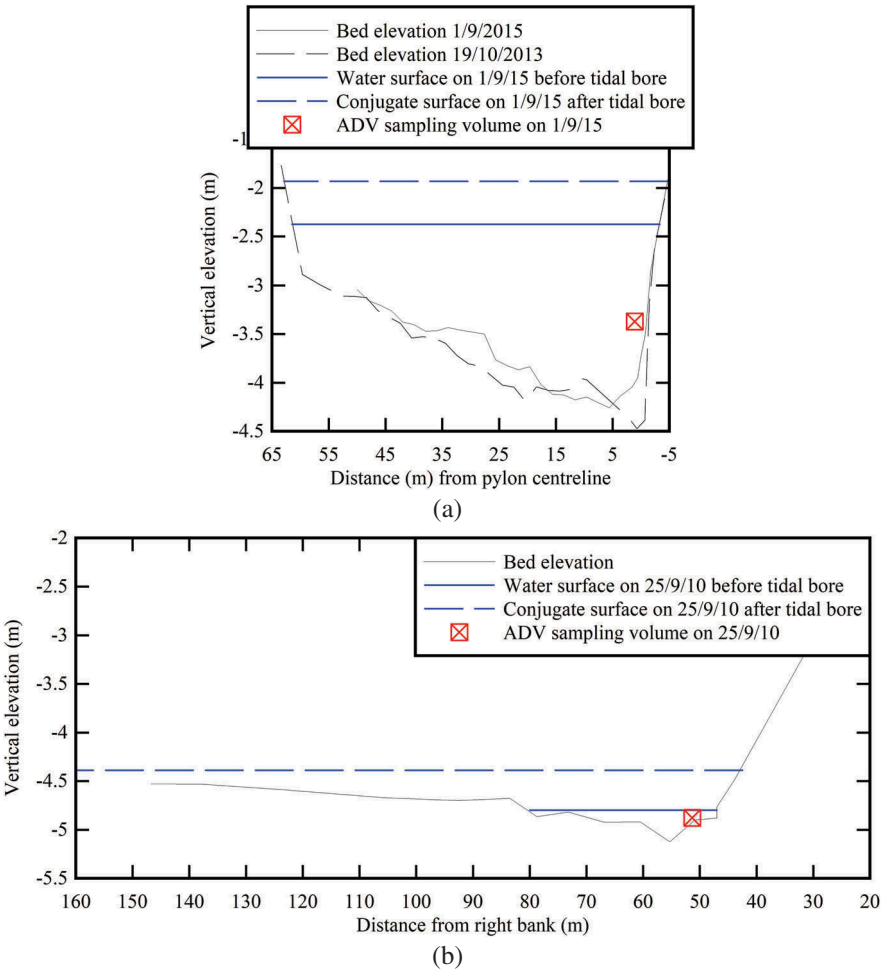

Figure 4. Surveyed channel cross sections looking downstream – bed elevation, free-surface elevation shortly prior to tidal bore and immediately after the bore front passage (conjugate depth).

(a) Garonne River tidal bore in the Arcins channel (France) on September 1 2015
(b) Sélune River tidal bore at La Pointe du Grouin du Sud, Bay of Mt St Michel (France) on September 25 2010

(Figure 3(a)) and propagated for the full length of the channel. At the sampling site (marked in Figure 3(c)), the tidal bore was undular: a series of free-surface undulations, with a wave period close to a second, followed the leading front and lasted for several minutes. The bore appearance is observed to differ in the Bay of Mt St Michel. The tidal bore occurred about 15 min before reaching the sampling location. The breaking bore presented a marked roller with a curved shape, viewed in elevation (Figure 3(b)). In the far background toward the left side of the channel (Figure 3(b)), the bore front propagated and overtopped on the dry sand banks and the waters were dark.

A key feature of all tidal bore is the rapid rise *Dd* in free-surface elevation, when the bore front passed. Typical data are reported in Table 2 (Column 12). The equations of conservation of mass and momentum may be developed in their integral form across the bore front. The result is an analytical solution in terms the ratio of conjugate cross-section areas A_2/A_1 as a function of the Froude number Fr_1 and cross-section shape (Chanson, 2012):

$$\frac{A_2}{A_1} = \frac{1}{2} \times \frac{\sqrt{\left(2 - \frac{B'}{B}\right)^2 + 8 \times \frac{\frac{B'}{B}}{\frac{B_1}{B}} \times {Fr_1}^2} - \left(2 - \frac{B'}{B}\right)}{\frac{B'}{B}} \quad (1)$$

where A_1 is the initial cross-section area, A_2 is the new cross-sections area: $A_2 = A_1 + DA$ immediately behind the bore front, B_1 is the initial free-surface width, B and B' are characteristic dimensions defined as:

$$B = \frac{A_2 - A_1}{d_2 - d_1} = \frac{\Delta A}{\Delta d} \quad (2)$$

$$B' = \frac{\int_{A_1}^{A_2} (d_2 - z) \times dA}{\frac{1}{2} \times (d_2 - d_1)^2} \quad (3)$$

with d_1 and d_2 the initial and new water depths. The tidal bore Froude number Fr_1 is defined as:

$$Fr_1 = \frac{V_1 + U}{\sqrt{g \times \frac{A_1}{B_1}}} \quad (4)$$

Table 2. Tidal bore properties in the Arcins channel (Garonne River, France) and La Pointe du Grouin du Sud (Sélune River, France) – comparison with cross-sectional and hydrodynamic properties of tidal bores during previous field measurements.

Reference	River	Date	Tidal range (m)	Bore type	Fr_1	U m/s	V_1 m/s	d_1 m	A_1 m^2	B_1 m	Dd m	DA m^2	B_2 m	B m	B' m	A_1/B_1	B_2/B_1	B/B_1	B'/B_1	A_2/A_1
Garonne 2010	Garonne River	September 10 2010	6.03	Undular	1.30	4.49	0.33	1.77	105.7	75.4	0.50	39.4	81.6	78.5	76.7	1.40	1.083	1.042	1.018	1.37
		September 11 2010	5.8	Undular	1.20	4.20	0.30	1.81	108.8	75.8	0.46	36.0	81.6	78.2	77.5	1.43	1.076	1.032	1.021	1.33
Sélune 2010	Sélune River	September 24 2010	9.8	Breaking	2.35	2.00	0.86	0.38	5.25	34.7	0.34	27.3	*116.9*	80.9	66.6	0.15	3.37	2.33	1.92	6.19
		September 25 2010	9.9	Breaking	2.48	1.96	0.59	0.33	3.56	33.2	0.41	31.3	*117.0*	77.3	65.7	0.11	3.53	2.33	1.98	9.79
Garonne 2012	Garonne River	June 7 2012	5.68	Undular (very flat)	*1.02*	*3.85*	0.68	2.72	158.9	79.0	0.45	36.71	84.3	81.6	82.4	2.00	1.067	1.033	1.043	1.233
		June 7 2012	5.5	Undular	1.19	4.58	0.59	2.65	152.3	78.7	0.52	42.24	84.3	81.2	81.8	1.94	1.071	1.032	1.040	1.278
Garonne 2013	Garonne River	October 19 2013	6.09	Undular	1.27	4.32	0.26	2.05	85.6	65.0	0.30	19.8	67.0	65.8	65.7	1.32	1.031	1.013	1.011	1.231
Garonne 2015	Garonne River	August 29 2015	5.85	Undular	1.18	4.23	0.29	1.685	101.4	67.6	0.338	23.24	69.9	68.9	68.4	1.50	1.034	1.019	1.012	1.23
		August 30 2015	6.17	Undular	1.34	4.25	0.21	1.25	72.8	64.3	0.470	30.72	67.4	65.4	65.5	1.13	1.048	1.017	1.019	1.42
		August 31 2015	6.22	Undular	1.70	4.79	0.18	1.122	56.6	65.1	0.496	33.30	69.5	67.2	66.7	0.87	1.068	1.032	1.025	1.59
		September 1 2015	6.04	Undular	1.38	4.45	0.22	1.28	74.9	64.5	0.440	29.07	67.6	66.1	65.6	1.16	1.048	1.024	1.017	1.39
		October 27 2015	6.32	Undular	1.33	4.61	0.22	1.24	88.0	65.9	0.480	32.23	69.1	67.2	67.0	1.34	1.049	1.019	1.017	1.37
Garonne 2016	Garonne River	November 14 2016	6.01	Undular	1.07	4.26	0.07	0.86	118.1	70.3	0.50	37.79	74.0	71.6	71.1	1.68	1.053	1.018	1.012	1.30
		November 15 2016	6.09	Undular	1.10	4.44	0.09	0.99	122.3	71.5	0.33	23.7	73.5	71.8	31.2	1.71	1.028	1.004	0.437	1.19
Wolanski et al. (2004)	Daly River	July 2 2003	~6	Undular	1.04	4.70	0.15	1.50	289.3	129.2	0.28	36.4	130.9	130.1	129.3	2.24	1.013	1.007	1.001	1.13
Simpson, Fisher, and Wiles (2004)	Dee River	September 6 2003	7.55	Breaking	1.79	4.1	0.15	0.72	39.3	68.3	0.45	31.4	72.8	70.4	74.1	0.58	1.066	1.030	1.085	1.80
Furgerot et al. (2013)	Sée River	May 7 2012	13.6	Undular	1.39	3.2	0.4	0.9	14.82	21.7	0.56	12.9	23.9	23.0	22.7	0.68	1.101	1.060	1.046	1.87

A_1: channel cross-section area immediately prior to the bore passage; B_1: free-surface width immediately prior to the bore passage; d_1: water depth next to ADV immediately prior to the bore passage; Fr_1: tidal bore Froude number (Equation (4)); U: tidal bore celerity positive upstream on the channel centerline; V_1: downstream surface velocity on the channel centerline immediately prior to the bore passage; *Italic data*: incomplete data.

with V_1 being the late ebb flow velocity (positive downstream), U being the bore celerity (also positive upstream), and g being the acceleration of gravity. Field observations are reported in Figure 5(a). The present data are compared to Equation (1) (open circles) and previous field data. In addition, the Bélanger equation is included:

$$\frac{A_2}{A_1} = \frac{1}{2} \times \left(\sqrt{1 + 8 \times Fr_1^2} - 1 \right) \quad (5)$$

Although, Equation (5) is only valid for a smooth rectangular channel. Figure 5(a) shows a satisfactory agreement between Equation (1) and *in situ* observations. The data are further reported in Table 2.

All field observations showed that the bore shape was related to the Froude number (Peregrine, 1966; Chanson, 2011a). A bore with a breaking front and marked roller was observed for $Fr_1 > 1.5$ to 1.7. For $1.3 < Fr_1 < 1.5$ to 1.7, the bore was undular with limited breaking: it was also called a breaking bore with secondary waves. And an undular bore, without breaking, was observed for $Fr_1 < 1.3$. A key aspect of undular bores was the smooth front followed by some secondary wave motion. Dimensionless wave amplitude and wave length data are plotted (Figure 5(b,c)), as well as listed in Table 2. In Figure 5(b,c), the present data are compared to past field data and analytical solutions: i.e. linear wave theory (Lemoine, 1948) and Boussinesq equations (Andersen, 1978). All undular bore data showed that the dimensionless wave amplitude $a_w/(A_1/B_1)$ increased with increasing Froude number for $1 < Fr_1 < 1.3$ to 1.4 (Figure 5(b)). The maximum wave amplitude corresponded to the appearance of wave breaking at the first wave crest. For $Fr_1 > 1.3$ to 1.4, the observations presented a trend with decreasing wave amplitude with increasing Froude number. For all Froude numbers, the undular wave length decreased with increasing Froude number, as seen in Figure 5(c). Overall the entire field data were relatively close, and the data trend was consistent with laboratory data and theoretical solutions.

A key feature of all field measurements conducted as part of the project MASCARET (Table 1) was the high temporal resolutions with continuous high-frequency water surface elevation and velocity measurements, starting prior to the tidal bore and extending

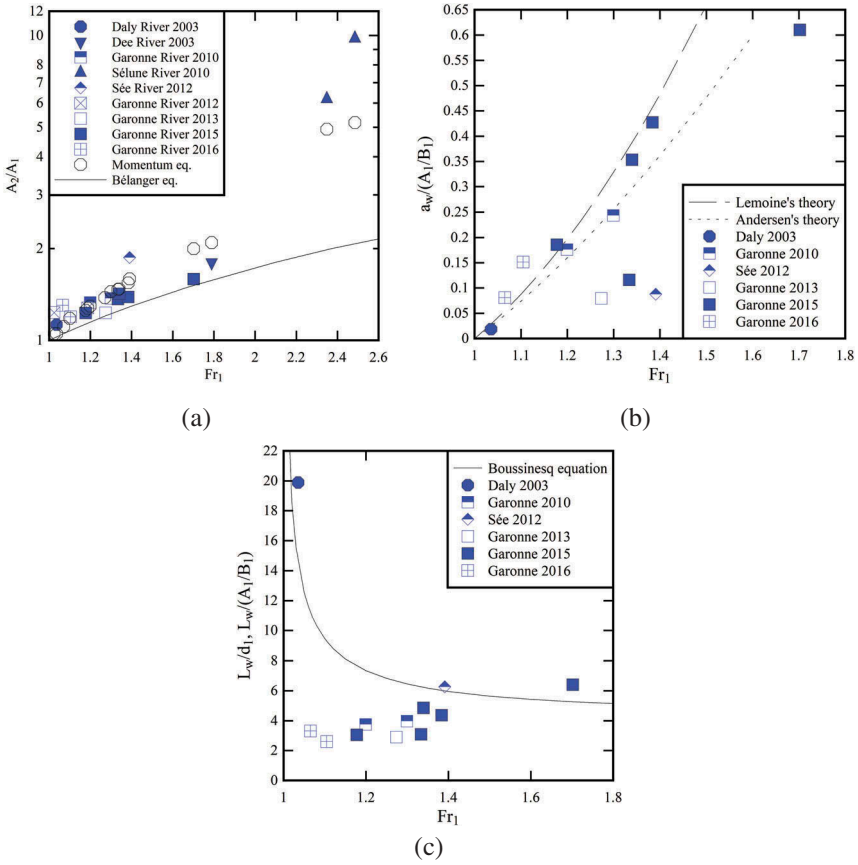

Figure 5. Free-surface characteristics of tidal bore field observations.

(a) Relationship between conjugate cross-sectional area ratio A_2/A_1 and Froude number Fr_1: comparison between field observations (blue symbols), momentum principle solution for an irregular channel (Equation (1), black hollow circles), and the Bélanger equation (Equation (5), solid line)
(b) Dimensionless wave amplitude $a_w/(A_1/B_1)$ of undular tidal bores – comparison between field observations (blue symbols, same legend as Figure 4(a)), linear wave theory (Lemoine, 1948), and Boussinesq equations (Andersen, 1978)
(c) Wave length $L_w/(A_1/B_1)$ of undular tidal bores – comparison between field observations and Boussinesq equation (Andersen, 1978) (Same legend as Figure 4(b))

for at least 1 h after the bore passage. The results showed a sharp flow deceleration associated with the bore passage, together with rapid and large fluctuations during and after the bore. Figure 6 presents a typical example for the Garonne River undular bore, and Figure 7 presents some observations in the Sélune River breaking bore. Figure 6(a) shows about a 3-h record of water depth and horizontal velocity component around the bore passage. Figures 6(b) and 7 present the temporal evolutions of water depth and all three velocity components during the bore front. Both graphs illustrate the rapid and large fluctuations of all three velocity components immediately after the surge passage, with both undular (Figure 6(b)) and breaking (Figure 7) bores.

The passage of the tidal bore front is always associated with a sharp rise in water level. The tidal bore is a shock, as it is a sharp discontinuity in terms of flow depth, pressure, velocity, and shear stress. The front is immediately followed by large and long-lasting fluctuations of water depth, as well as both velocity and shear stress. All velocity data exhibited a fast deceleration during the passage of the bore, as illustrated in Figures 6 and 7. In Figure 6(b), the longitudinal deceleration is about −0.35 m/s^2 at 18:52 on September 1 2015. For comparison, the deceleration was −1.6 m/s^2 in the breaking bore of the Sélune River (Figure 7). Except on June 7 2012, the bore passage was associated with an immediate change in flow direction: i.e. $V_x < 0$ after the bore. The passage of

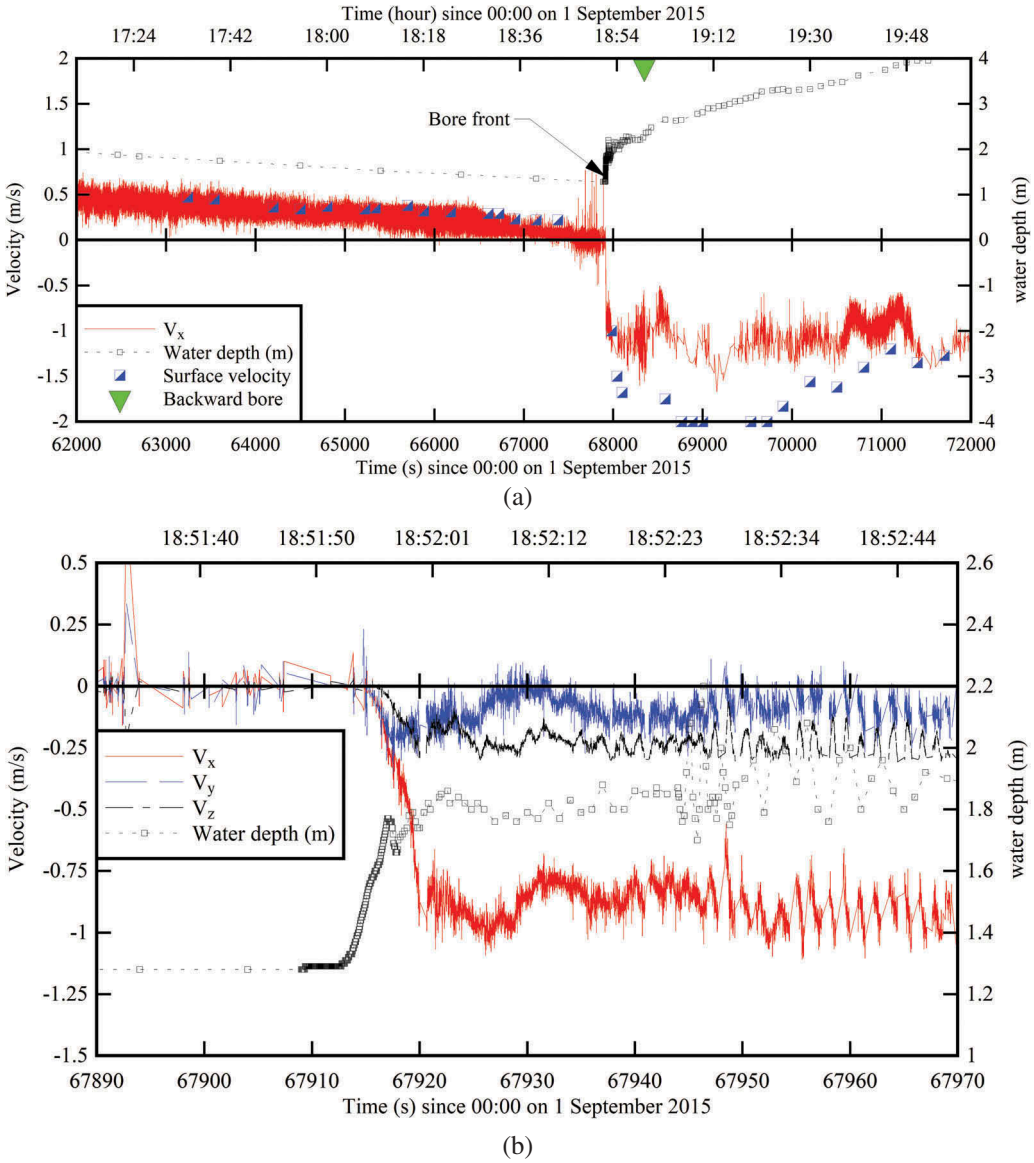

Figure 6. Time-variations of water depth and instantaneous velocity components during the Arcins channel tidal bore on September 1 2015.

(a) Water depth and longitudinal velocity – Surface velocities were recorded on the channel centerline – Green triangle (Backward bore) indicates time of passage of backward bore at sampling site

(b) Velocity components about the passage of the tidal bore

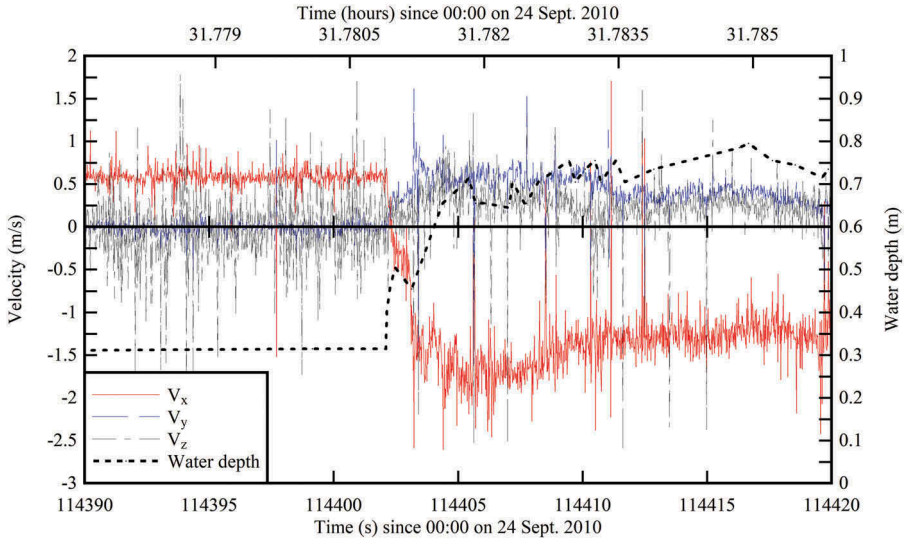

Figure 7. Time variations of water depth and instantaneous velocity components during the Sélune River tidal bore on September 25 2010 about the passage of the tidal bore.

the bore was further associated with relatively-long-period oscillations superposed to high-frequency turbulence. The former was linked to the generation of large-scale coherent vortices and their upstream advection behind the tidal bore.

The unsteady turbulent flow motion exhibits large instantaneous turbulent Reynolds stresses beneath the bore front and very-early flood tide motion. In the Garonne and Sélune River tidal bores, the data indicated maximum instantaneous normal shear stresses in excess of 150 Pa and maximum instantaneous tangential stress magnitudes up to 100 Pa. The instantaneous turbulent shear stresses exceeded the critical threshold for motion and transport of fine cohesive and non-cohesive sediments. Large-scale eddies played a key role for sediment pick-up and saltation, and sediment motion driven by convection occurred because the turbulent length scale was much larger than the sediment characteristic dimension (Nielsen, 1992; Chanson, 1999).

All field data systematically highlighted the intensity of turbulent mixing induced by tidal bores, combined with accretion and deposition of sediments in the upper estuarine zones. This was evidenced by the hyper-concentration of the flow immediately after the tidal bore passage (Chanson et al., 2011; Keevil, Chanson, and Reungoat, 2015; Furgerot et al., 2016; Reungoat, Leng, and Chanson, 2017). Typical SSC data are plotted in Figure 8(a), showing time variations of instantaneous SSC estimates, derived from ADV signal amplitude, and SSC data measured from water samples collected during the study. For the same tidal bore event, Figure 8(b) presents the characteristic grain sizes of the sediment suspensions. In Figure 8, the passage of the bore and rapid flow deceleration are followed by large suspended sediment levels, with comparable results between water samples collected at the water surface and SSC estimate recorded in the water column. The SSC estimate record shows further rapid and large fluctuations in sediment concentrations. During the early flood tide, i.e. $0 < t - T_{bore} < 2$ h, visual observations highlighted intense interactions between turbulence and sediment advection, with fascinating patches of sediment upwelling at the free surface, originating from the bed. The boundaries of each patch were well defined, with a sharp concentration gradient across the interfaces, and the mixing occurred very slowly as the differences in color can be observed. The sizes of surface structures and scars would vary from 0.1 to 10 m in the Arcins channel, which is 70 m wide. Once reaching the free surface, these patches were then transported upstream by the flood tide motion.

4. Discussion

The present field observations, combined with personal tidal bore observations by the authors in several other systems, showed a number of common features to all tidal bores in natural systems. At the same time, these observations revealed specific features, rarely seen in laboratory, as well as the uniqueness of each event, with both spatial and temporal evolutions.

A tidal bore is basically generated by a large tidal range, with longitudinal maximum (tidal range) greater than 4–6 m in the estuarine zone (Tricker, 1965; Chanson, 2011a). The development and onset to tidal bore can be modeled by shallow water equations including the Saint-Venant equations and the method of characteristics (Barré de Saint-Venant, 1871a, 1871b; Liggett and Cunge, 1975). At a given instant, the tidal bore is the most upstream extent of the food tide in a tidal bore affected estuarine zone. A tidal bore is never observed during the ebb tide.

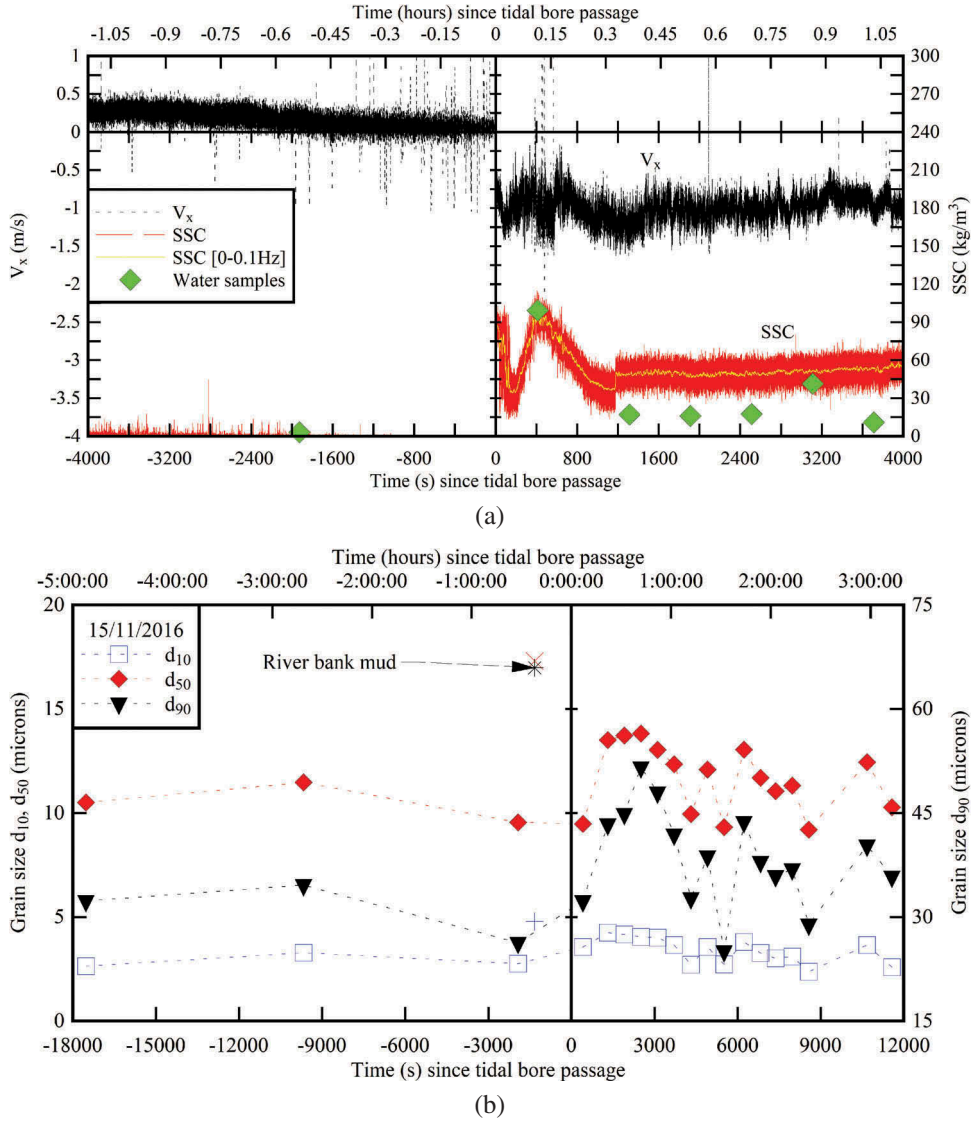

Figure 8. Suspended sediment characteristics in the Garonne River tidal bore on November 15 2016.

(a) Time variations of the suspended sediment concentrations of water samples (solid symbols) and instantaneous suspended sediment concentration estimates – instantaneous SSC in red and mean (low-pass filtered) SSC in yellow – comparison with the instantaneous suspended longitudinal velocity component

(b) Time variations of the characteristic grain sizes d_{10}, d_{50}, and d_{90} – comparison with the river bank mud median grain sizes (cross and asterisk symbols) – note the different vertical scales for d_{10} and d_{50} (left vertical axis) and d_{90} (right vertical axis)

Physically the bore is a positive surge, compression wave, and hydraulic jump (in translation) characterized by a net mass flux during the bore passage (Tricker, 1965; Lighthill, 1978). The momentum and continuity principles may be applied in an integral form to a control volume in translation with the bore front (Henderson, 1966; Lighthill, 1978; Liggett, 1994; Chanson, 2012). The application to the bore front provides a relationship between the initial flow conditions, new flow conditions, and bore celerity (Equation (1)).

For a breaking bore, the bore celerity is not truly constant, but it constantly fluctuates about a mean value (Leng and Chanson, 2015a). The fluctuations in bore celerity are large in both transverse and longitudinal directions, with ratio of standard deviation to mean value greater than unity. The bore roller toe perimeter fluctuates rapidly with time and space: that is, it is not a straight line in both laboratory and field (Chanson, 2016; Wang, Leng, and Chanson, 2017). A breaking tidal bore creates further a loud roaring noise that can be heard from far away (Moore, 1888). Noises are generated near the banks and in the breaking roller. It is believed that air entrapped and entrained in large-scale structures of the roller is acoustically active and contributes to the rumbling sound generation (Chanson, 2009, 2016).

The tidal bore propagation induces some very strong mixing (Hornung, Willert, and Turner, 1995; Chanson et al., 2011). Tidal bores have a major impact in terms of sediment transport (Simpson, Fisher, and Wiles, 2004; Furgerot et al., 2016), as documented *in situ* and in laboratory (Khezri and Chanson, 2012, 2015; Furgerot, 2014; Keevil, Chanson, and Reungoat, 2015), including

with losses of equipment buried beneath the bed sediments after the bore passage.

5. Specific features in natural systems

In the field, a tidal bore is a multiphase flow. The bore motion is a three-phase flow: liquid (water), solid (sediment), and gas (air), as illustrated by numerous photographs and illustrations (Figure 1). The three-phase nature of tidal bore flow was never accounted for, and the scientific literature is limited (Chanson, 2013; Leng and Chanson, 2015b). Most tidal bore occurrences are characterized by large sediment load and the turbulent processes in sediment-laden flows become a relevant factor (Jhia and Bombardelli, 2009). To date, the three-phase flow with high sediment and air content has never been investigated, despite the high practical relevance to tidal bore motion.

During the bore passage and immediately after, the very early flood tide flow is a form of hyper-concentrated flow, with SSCs between 5 and 120 kg/m^3. Such SSC levels would correspond to volume concentrations between 0.2% and 4.6%. With bentonite suspensions with 2% volume concentration, Chanson, Jarny, and Coussot (2006) demonstrated a non-Newtonian thixotropic flow behavior during both dam break wave experiment and rheometry tests. Based upon direct magnetic resonance imaging tests, Coussot and Ovarlez (2010) clearly showed a non-Newtonian thixotropic behavior with bentonite suspensions with volume concentrations from 3% to 7%. During tidal bore field studies, detailed observations in the Garonne River indicated high SSC levels and rheological data, which combined to suggest a non-Newtonian flow behavior (Chanson et al., 2011; Reungoat, Chanson, and Caplain, 2014; Reungoat, Leng, and Chanson, 2017; Keevil, Chanson, and Reungoat, 2015). Such hyper-concentrated non-Newtonian flow behavior was rarely documented and never accounted for in modeling. Suspended sediments are believed to be one cause of repeated instrumentation issues. With ADV systems, the importance of settings on velocity signal quality was reported by Chanson et al. (2010), Mouaze, Chanson, and Simon (2010), and Furgerot (2014), while Reungoat, Leng, and Chanson (2016) documented the effects of ADV power settings on SSC estimate calibration.

During a given flood tide, the tidal bore presents unique features at each site along the estuary. Spatial variations of a tidal bore are very common during a flood tide. The bore shape changes in response to changes in bathymetry in natural channels. This aspect is well documented in well-known systems (Rowbotham, 1983; Chanson, 2011a). This aspect is rarely observed in laboratory albeit a few exceptions (Chanson, 2011b; Kiri, Leng, and Chanson, 2017). Further, at a given site, a tidal bore appearance changes from flood tide to flood tide and the bore may exhibit distinctively different features. Small diurnal inequality can also induce substantial changes in the bore appearance and properties.

During field studies, a number of unusual observations were documented. These include some delayed flow reversal, for example, in the Seine River (Bazin, 1865), in the Rio Mearim, Brazil (Kjerfve and Ferreira, 1993), in the Garonne River in June 2012 (Reungoat, Chanson, and Caplain, 2014). In these situations, the flow direction reversal took place a minute to a few minutes after the passage of the bore front. Other anecdoctic observations were report of "backward" bores and bore collision. The former means tidal bores propagating downstream, which might sometimes impact onto incoming bores. These processes were observed in braided channels, when the tidal bore in one channel would travel faster than in another, enter the upstream end of the other channel, and travel downstream. "Backward" bores were well documented in the Garonne River at Arcins (Reungoat, Chanson, and Caplain, 2014; Reungoat, Leng, and Chanson, 2016; Keevil, Chanson, and Reungoat, 2015), as well as observed in the Severn River, UK (Rowbotham, 1983), Trent River, UK (as mentioned to Hubert Chanson from Eric Jones (2012)), and Digul River, Indonesia (as mentioned to Hubert Chanson from Antony Colas (2015)). A man-made bore collision occurred in the Petitcodiac River (Canada) when an upstream reservoir release propagated downstream, colliding frontally with the incoming tidal bore (CBC News, 2013, as mentioned to Hubert Chanson from Daniel Leblanc (2013)). Bestehorn and Tyvand (2009) proposed an analytical solution. In the Garonne River field studies, this "backward" bore did not produce any detected change in the sediment transport (Figure 6(b)). During the very early flood tidal flow, the sediment transport would continue to flow upstream, in addition to very-localized sediment bursting in the deeper sections of the channel. The latter produced sediment flocs flowing up to the free surface, typically within the first hour after tidal bore passage.

At a given site, the successive occurrence of tidal bores over several consecutive days may yield a progressively broader grain size distribution, as well as some increase in median sediment size from day one onwards (Reungoat, Leng, and Chanson, 2017). This is associated with a gradual increase in initial mean SSC estimate prior to the bore. The initial river bed scouring by the tidal bore, and deposition occurring subsequently during the late flood tide and ebb tide, can contribute to longitudinal sediment mixing between all sediments sources, thus modifying over time the bed material composition.

6. Conclusion and future research

Recent *in situ* observations prove that the tidal bore Froude number is a most defining criterion of analysis.

Field measurements indicate large fluctuations in bore celerity in transverse and longitudinal directions, which were rarely documented until very recently. Very large instantaneous Reynolds stresses are consistently observed during and shortly after tidal bores, with amplitudes up to 150 Pa. These shear stress amplitudes are one to two orders of magnitude larger than the critical threshold for sediment pick-up and motion, and sediment transport is always very intense behind tidal bores, generating hyper-concentrated flows.

Even when common trends can be highlighted for tidal bores, all field observations confirm that very complicated and local flow features are associated with a tidal bore propagation, making each tidal bore almost unique and relevant to the place where it has been observed. Macro-turbulent events, likely induced by some secondary motion, are observed in natural rivers, induced by the bore front and flow reversal with some very-energetic turbulent events. The Garonne River morphology, like any other river, is very irregular, and large macro-recirculations are generated by meanders, which are then advected by the river stream. Moreover, the three-dimensional bathymetry generates hydrodynamic structures at the bed, which can be related to kolk and boils or bursting events ejected upwards from the three-dimensional river bed macro-irregularities.

The three-phase nature of tidal bore flow has been well documented by numerous photographs and movies. Future research should focus on the multiphase flow characteristics and the interactions between the three phases: liquid (water), solid (sediment), and gas (air).

Acknowledgments

The authors thank all the people who participated to the field works, without whom the study could not have been conducted. They acknowledge the assistance of Patrice Benghiati and the permission to access and use the pontoon in the Bras d'Arcins (France), as well as the assistance of Jean-Yves Cocaign, Écomusée de la Baie du Mont Saint-Michel (France). They further thank Frédéric Daney and Antony Colas (France) for a number of useful discussions on their surfing experiences. PL, XL, and HC thank Prof. Dong-zi Pan (ZIHE, China), Dr Frederique Larrarte, Dr Dominique Mouaze, Dr Bernadette Tessier (France), and Dr Eric Jones (UK) for helpful exchanges. The financial support through the Agence Nationale de la Recherche (Project MASCARET ANR-10-BLAN-0911) and Australian Research Council (Grant DP120100481) is acknowledged.

Disclosure statement

No potential conflict of interest was reported by the authors.

Funding

This work was supported by the Agence Nationale de la Recherche [Project MASCARET ANR-10-BLAN-0911] and Australian Research Council [DP120100481].

ORCID

Pierre Lubin http://orcid.org/0000-0003-1957-6854
Xinqian Leng http://orcid.org/0000-0001-8472-7925
Hubert Chanson http://orcid.org/0000-0002-2016-9650

References

Andersen, V. M. 1978. "Undular Hydraulic Jump." *Journal of Hydraulic Division, ASCE* 104 (HY8): 1185–1188. Discussion: Vol. 105, No. HY9, pp. 1208–1211.

Barré de Saint-Venant, A. J. C. 1871a. "Théorie du Mouvement Non Permanent des Eaux, avec Application aux Crues des Rivières et à l'Introduction des Marées dans leur Lit." In *Comptes Rendus des séances de l'Académie des Sciences* (in French), 147–154. Vol. 73, No. 4. Paris, France: French Academy of Sciences.

Barré de Saint-Venant, A. J. C. 1871b. "Théorie et Equations Générales du Mouvement Non Permanent des Eaux, avec Application aux Crues des Rivières et à l'Introduction des Marées dans leur Lit (2ème Note)." In *Comptes Rendus des séances de l'Académie des Sciences* (in French), 237–240. Séance 17 July 1871, Vol. 73. Paris, France: French Academy of Sciences.

Bartsch-Winkler, S., and D. K. Lynch. 1988. "Catalog of Worldwide Tidal Bore Occurrences and Characteristics." In *US Geological Survey Circular, No. 1022*, 17. Virigina, US: US Geological Survey (USGS).

Bazin, H. 1865. "Recherches Expérimentales sur la Propagation des Ondes." ('Experimental Research on Wave Propagation.')." In *Mémoires présentés par divers savants à l'Académie des Sciences* (in French), 495–644. Vol. 19. Paris, France: French Academy of Sciences.

Bestehorn, M., and P. A. Tyvand. 2009. "Merging and Colliding Bores." *Physics of Fluids* 21: 042107, 11 pages. doi:10.1063/1.3115909.

Chanson, H. 1999. "The Hydraulics of Open Channel Flow: An Introduction" In *Butterworth-Heinemann*, 1st. London, UK: 512.

Chanson, H. 2009. "The Rumble Sound Generated by a Tidal Bore Event in the Baie Du Mont Saint Michel." *Journal of the Acoustical Society of America* 125 (6): 3561–3568. doi:10.1121/1.3124781.

Chanson, H. 2011a. "Tidal Bores, Aegir, Eagre, Mascaret, Pororoca: Theory and Observations." In *World Scientific*, 220. Singapore.

Chanson, H. 2011b. "Undular Tidal Bores: Effect of Channel Constriction and Bridge Piers." *Environmental Fluid Mechanics* 11 (4): 385–404. 4 videos. doi: 10.1007/s10652-010-9189-5.

Chanson, H. 2012. "Momentum Considerations in Hydraulic Jumps and Bores." *Journal of Irrigation and Drainage Engineering, ASCE* 138 (4): 382–385. doi:10.1061/(ASCE)IR.1943-4774.0000409.

Chanson, H. 2013. "Hydraulics of Aerated Flows: Qui Pro Quo?" *Journal of Hydraulic Research* 51 (3): 223–243. IAHR, Invited Vision paper. doi: 10.1080/00221686.2013.795917.

Chanson, H. 2016. "Atmospheric Noise of a Breaking Tidal Bore." *Journal of the Acoustical Society of America* 139 (1): 12–20. doi:10.1121/1.4939113.

Chanson, H., S. Jarny, and P. Coussot. 2006. "Dam Break Wave of Thixotropic Fluid." *Journal of Hydraulic Engineering, ASCE* 132 (3): 280–293. doi:10.1061/(ASCE)0733-9429(2006)132:3(280).

Chanson, H., P. Lubin, B. Simon, and D. Reungoat (2010). "Turbulence and Sediment Processes in the Tidal Bore of the Garonne River: First Observations." *Hydraulic Model Report No. CH79/10*, School of Civil Engineering, The University of Queensland, Brisbane, Australia, 97.

Chanson, H., D. Reungoat, B. Simon, and P. Lubin. 2011. "High-Frequency Turbulence and Suspended Sediment Concentration Measurements in the Garonne River Tidal Bore." *Estuarine Coastal and Shelf Science* 95 (2–3): 298–306. doi:10.1016/j.ecss.2011.09.012.

Coussot, P., and G. Ovarlez. 2010. "Physical Origin of Shear-Banding in Jammed Systems." *European Physics Journal E* 33 (3): 183–188. doi:10.1140/epje/i2010-10660-9.

de LA CONDAMINE, C. M. (1745). "Relation abrégée d'un voyage fait dans l'intérieur de l'Amérique méridionale, depuis la côte de la mer du sud jusqu'aux côtes du Brésil et de la Guyane, en descendant la rivière des Amazones." *J.E.DUFOUR and P. ROUX Libraires*, 415. Maestricht, (in French).

Faas, R. W. (1995). "Rheological Constraints on Fine Sediment Distribution and Behavior: The Cornwallis Estuary, Novia Scotia." *Proc. Canadian Coastal Conference*, Dartmouth, Nova Scotia, pp. 301–314.

Fan, D., J. Tu, S. Shang, and G. Cai. 2014. "Characteristics of Tidal-Bore Deposits and Facies Associations in the Qiantang Estuary, China." *Marine Geology* 348: 1–14. doi:10.1016/j.margeo.2013.11.012.

Fan, D. D., G. F. Cai, Y. J. Wu, Y. W. Zhang, and L. Gao. 2012. "Sedimentation Processes and Sedimentary Characteristics of the North Bank of the Qiantang Estuary." *Chinese Science Bulletin* 57 (13): 1578–1589. doi:10.1007/s11434-012-4993-6.

Furgerot, L. (2014). "Propriétés hydrodynamiques du mascaret et de son influence sur la dynamique sédimentaire. Une approche couplée en canal et in situ (estuaire de la Sée, Baie du Mont Saint Michel)." *Ph.D. thesis*, University of Caen Basse-Normandie, France, 386(in French).

Furgerot, L., D. Mouaze, B. Tessier, L. Perez, and S. Haquin (2013). "Suspended Sediment Concentration in Relation to the Passage of a Tidal Bore (Sée River Estuary, Mont Saint Michel, NW France)." *Proc. Coastal Dynamics 2013*, Arcachon, France, 24–28 June, pp. 671–682.

Furgerot, L., D. Mouaze, B. Tessier, L. Perez, S. Haquin, P. Weill, and A. Crave. 2016. "Sediment Transport Induced by Tidal Bores. An Estimation from Suspended Matter Measurements in the Sée River (Mont-Saint-Michel Bay, Northwestern France)." *Comptes Rendus Géoscience* 348: 432–441. doi:10.1016/j.crte.2015.09.004.

Greb, S. F., and A. W. Archer. 2007. "Soft-Sediment Deformation Produced by Tides in a Meizoseismic Area, Turnagain Arm, Alaska." *Geology* 35 (5): 435–438. doi:10.1130/G23209A.1.

Henderson, F. M. 1966. "Open Channel Flow." In *MacMillan Company*. New York, USA.

Hornung, H. G., C. Willert, and S. Turner. 1995. "The Flow Field Downsteam of a Hydraulic Jump." *Journal of Fluid Mechanisms* 287: 299–316. doi:10.1017/S0022112095000966.

Jhia, S. K., and F. A. Bombardelli. 2009. "Two-Phase Modelling of Turbulence in Dilute Sediment-Laden, Open Channel Flows." *Environmental Fluid Mechanics* 9: 237–266. doi:10.1007/s10652-008-9118-z.

Keevil, C. E. (2016). "Barscale Morphodynamics through the Tidal-Fluvial Transition." *Ph.D. thesis*, University of Hull, UK, 234

Keevil, C. E., H. Chanson, and D. Reungoat. 2015. "Fluid Flow and Sediment Entrainment in the Garonne River Bore and Tidal Bore Collision." *Earth Surface Processes and Landforms* 40 (12): 1574–1586. doi:10.1002/esp.3735.

Khezri, N., and H. Chanson. 2012. "Sediment Inception under Breaking Tidal Bores." *Mechanics Research Communications* 41: 49–53. 1 video movie. doi:10.1016/j.mechrescom.2012.02.010).

Khezri, N., and H. Chanson. 2015. "Turbulent Velocity, Sediment Motion and Particle Trajectories under Breaking Tidal Bores: Simultaneous Physical Measurements." *Environmental Fluid Mechanics* 15 (3): 633–651. doi:10.1007/s10652-014-9358-z.

Kiri, U., X. Leng, and H. Chanson (2017). "Positive Surge Propagation in Non-Rectangular Channels." *Proceedings of 13th Hydraulics in Water Engineering Conference HIWE2017*, Engineers Australia, Sydney, 13–16 November, 9.

Kjerfve, B., and H. O. Ferreira. 1993. "Tidal Bores: First Ever Measurements." *Ciência E Cultura (Jl of the Brazilian Assoc. For the Advancement of Science)* 45 (2, March/April): 135–138.

Lemoine, R. 1948. "Sur Les Ondes Positives De Translation Dans Les Canaux Et Sur Le Ressaut Ondulé De Faible Amplitude." ('On the Positive Surges in Channels and on the Undular Jumps of Low Wave Height.')." In *Jl La Houille Blanche (In French)*, 183–185.

Leng, X., and H. Chanson. 2015a. "Breaking Bore: Physical Observations of Roller Characteristics." *Mechanics Research Communications* 65: 24–29. doi:10.1016/j.mechrescom.2015.02.008.

Leng, X., and H. Chanson. 2015b. "Turbulent Advances of a Breaking Bore: Preliminary Physical Experiments." *Experimental Thermal and Fluid Science* 62: 70–77. doi:10.1016/j.expthermflusci.2014.12.002.

Lewis, A. W. (1972). "Field Studies of a Tidal Bore in the River Dee." *M.Sc. thesis*, Marine Science Laboratories, University College of North Wales, Bangor, UK.

Liggett, J. A. 1994. *Fluid Mechanics*. New York, USA: McGraw-Hill.

Liggett, J. A., and J. A. Cunge. 1975. "Numerical Methods of Solution of the Unsteady Flow Equations." In "Unsteady Flow in Open Channels."." In *WRP Publ.*, edited by K. Mahmood and V. Yevdjevich, 89–182. Vol. 1. Fort Collins, USA.

Lighthill, J. 1978. *Waves in Fluids*, 504. Cambridge, UK: Cambridge University Press.

Lynch, D. K. 1982. "Tidal Bores." *Scientific American* 247 (4): 134–143. doi:10.1038/scientificamerican1082-146.

Malandain, J. J. (1988). "La Seine Au Temps Du Mascaret." ('The Seine River at the Time of the Mascaret.') *Le Chasse-Marée* (in French), No. 34, pp. 30–45.

Manzano Manzono, J., and A. M. Manzano Fernandez Heredia. 1988. "Los Pinzones y el Descubrimiento de America." In *Ediciones De Cultura Hispanica*, Madrid, Spain: Instituto de Cooperacion Iberoamericana. 3 volumes (in Spanish).

Moore, W. U. (1888). "Report on the Bore of the Tsien-Tang Kiang." *Hydrographic Office*, London, 50 pages & 1 map.

Mouaze, D., H. Chanson, and B. Simon (2010). "Field Measurements in the Tidal Bore of the Sélune River in the Bay of Mont Saint Michel (September 2010)." *Hydraulic Model Report No. CH81/10*, School of Civil Engineering, The University of Queensland, Brisbane, Australia, 72.

Moule, A. C. 1923. "The Bore on the Ch'ien-T'ang River in China." *T'oung Pao* 22: 10–188. Archives pour servir à l'étude de l'histoire, des langues, la geographie et l'ethnographie de l'Asie Orientale (Chine, Japon, Corée, Indo-Chine, Asie Centrale et Malaisie). doi:10.1163/156853223X00104.

Navarre, P. (1995). "Aspects Physiques Du Caractère Ondulatoire Du Macaret En Dordogne." ('Physical Features of the Undulations of the Dordogne River Tidal Bore.') *D.E.A. thesis*, Univ. of Bordeaux, France, 72. (in French).

News, C. B. C. (2013). "5 Super Bore Surfers Hit by Surprise Wave in Moncton." Accessed 2 December 2013. {http://www.cbc.ca/news/canada/new-brunswick/5-super-bore-surfers-hit-by-surprise-wave-inmoncton-1.2418096}

Nielsen, P. 1992. "Coastal Bottom Boundary Layers and Sediment Transport." In *Advanced Series on Ocean Eng*. Vol. 4. Singapore: World Scientific Publ.

Pan, D. Z., and H. Chanson. 2015. "Physical Modelling of Tidal Bore Dyke Overtopping: Implication on Individuals' Safety." In *Proc. 36th IAHR World Congress*, 3824–3831. The Netherlands: Hague. 27 June-3 July. Theme 4.

Partiot, M. 1861. "Mémoire sur le Mascaret." In *Annales des ponts et chaussées*. Mémoires et documents relatifs à l'art des constructions et au service de l'ingénieur, 4èm Série, 1er Semestre, pp. 2–48 & 3 plates (in French).

Peregrine, D. H. 1966. "Calculations of the Development of an Undular Bore." *Journal Fluid Mechanisms* 25: 321–330. doi:10.1017/S0022112066001678.

Pouv, K. S., A. Besq, S. S. Gullou, and E. A. Toorman. 2014. "On Cohesive Sediment Erosion: A First Experimental Study of the Local Processes Using Transparent Model Materials." *Advances in Water Resources* 72: 71–83. doi:10.1016/j.advwatres.2014.05.012.

Reungoat, D., H. Chanson, and B. Caplain. 2014. "Sediment Processes and Flow Reversal in the Undular Tidal Bore of the Garonne River (France)." *Environmental Fluid Mechanics* 14 (3): 591–616. doi:10.1007/s10652-013-9319-y.

Reungoat, D., X. Leng, and H. Chanson (2016). "Hydrodynamic and Sedimentary Processes of Tidal Bores: Arcins Channel, Garonne River in August-September-October 2015." *Hydraulic Model Report No. CH102/16*, School of Civil Engineering, The University of Queensland, Brisbane, Australia, 270.

Reungoat, D., X. Leng, and H. Chanson. 2017. "Successive Impact of Tidal Bores on Sedimentary Processes: Arcins Channel, Garonne River." *Estuarine Coastal and Shelf Science* 188: 163–173. doi:10.1016/j.ecss.2017.02.025.

Reungoat, D., X. Leng, and H. Chanson (2017b). "Suspended Sediment Processes in the Garonne River Tidal Bore: Arcins Channel on 14–15 November 2016." Hydraulic Model Report No. CH108/17, School of Civil Engineering, The University of Queensland, Brisbane, Australia, 166. (ISBN 978-1-74272-187-3).

Rowbotham, F. 1983. *The Severn Bore*, 104. 3rd edition ed. Newton Abbot, UK: David & Charles.

Simpson, J. H., N. R. Fisher, and P. Wiles. 2004. "Reynolds Stress and TKE Production in an Estuary with a Tidal Bore." *Estuarine, Coastal and Shelf Science* 60 (4): 619–627. doi:10.1016/j.ecss.2004.03.006.

Tricker, R. A. R. 1965. *Bores, Breakers, Waves and Wakes*. New York, USA: American Elsevier Publ.

Tu, J., and D. Fan. 2017. "Flow and Turbulence Structure in a Hypertidal Estuary with the World's Biggest Tidal Bore." *Journal of Geophysical Research: Oceans, AGU* 122: 3417–3433. doi:10.1002/2016JC012120.

Vernes, J. 1881. *La Jangada. Huit cent lieues sur l'Amazone*. Paris, France: Hetzel.

Wang, H., X. Leng, and H. Chanson. 2017. "Bores and Hydraulic Jumps. Environmental and Geophysical Applications." *Engineering and Computational Mechanics, Proceedings of the Institution of Civil Engineers, UK* 170 (EM1): 25–42. doi:10.1680/jencm.16.00025.

Wolanski, E., D. Williams, S. Spagnol, and H. Chanson. 2004. "Undular Tidal Bore Dynamics in the Daly Estuary, Northern Australia." *Estuarine, Coastal and Shelf Science* 60 (4): 629–636. doi:10.1016/j.ecss.2004.03.001.

Xie, D. F., and C. H. Pan. 2013. "A Preliminary Study of the Turbulence Features of the Tidal Bore in the Qiantang River, China." *Journal of Hydrodynamics* 25 (6): 903–911. doi:10.1016/S1001-6058(13)60439-4.